How to cite: *Angew. Chem. Int. Ed.* **2021**, *60*, 5323–5330
International Edition: doi.org/10.1002/anie.202013899
German Edition: doi.org/10.1002/ange.202013899

Structure Elucidation

Unlocking the Water Trimer Loop: Isotopic Study of Benzophenone-$(H_2O)_{1–3}$ Clusters with Rotational Spectroscopy

*Weixing Li, María Mar Quesada-Moreno, Pablo Pinacho, and Melanie Schnell**

Abstract: *Examined here are the structures of complexes of benzophenone microsolvated with up to three water molecules by using broadband rotational spectroscopy and the cold conditions of a molecular jet. The analysis shows that the water molecules dock sideways on benzophenone for the water monomer and dimer moieties, and they move above one of the aromatic rings when the water cluster grows to the trimer. The rotational spectra shows that the water trimer moiety in the complex adopts an open-loop arrangement. Ab initio calculations face a dilemma of identifying the global minimum between the open loop and the closed loop, which is only solved when zero-point vibrational energy correction is applied. An OH···π bond and a Bürgi-Dunitz interaction between benzophenone and the water trimer are present in the cluster. This work shows the subtle balance between water–water and water–solute interactions when the solute molecule offers several different anchor sites for water molecules.*

Introduction

The way how molecules interact with each other to form molecular clusters is governed by the interplay between different kinds of noncovalent interactions. One important aspect of the process of aggregation is that several noncovalent interactions can operate simultaneously, and even small changes can tip the balance towards one or the other preferred binding scheme.[1,2] Thus, knowledge of how noncovalent interactions manifest themselves and how they compete and cooperate with each other in small molecular clusters can be essential for a comprehension of molecular aggregation.

There is a long-lasting effort to qualitatively and quantitatively understand the intermolecular interactions of water, since it is a remarkable substance of great importance for life. Water's chemical-physical properties and its role in biological processes arise from its outstanding capability to form interactions,[3] and water clusters are favored model systems to investigate these inter-water interactions. Back in the 1960s, Morokuma and Pedersen[4] and Kollman and Allen[5] were the first to study the hydrogen bond (HB) between water molecules with ab initio Hartree–Fock calculations. Hankins and co-workers investigated the interaction potential for the water dimer and trimer in 1970.[6] Experimentally, the structures of isolated water clusters of increasing size in the gas phase are still of interest today[7–17] since the first experimental study of the water dimer.[7] Recently, Pérez et al. have employed broadband rotational spectroscopy to determine the structures of different isomers of water clusters up to the water nonamer and decamer using a pulsed molecular jet expansion.[17] Water self-association is dominated by intermolecular HBs. However, when interacting with solute molecules, other noncovalent interactions may appear and alter the structures of water clusters. The characterization of these systems provides new insight into solvation phenomena such as the spectroscopic study of the structures of benzene-$(H_2O)_n$ clusters.[18,19] Thus, it is important to identify the structures not only of pure water clusters, but also of solvated complexes.

Rotational spectroscopy is a method with high resolution and especially useful to determine molecular structures since rotational spectra are highly sensitive to changes in the moments of inertia and thus in the overall mass distribution of the molecules.[20] The two main requirements for rotational spectroscopy are that the experiment needs to be performed in the gas phase and that the molecules or molecular clusters are polar. Combining rotational spectroscopy with the supersonic jet technique allows us to generate and study weakly bound complexes. Typically, the analysis of rotational spectra is supported by quantum-chemical calculations.

The smallest cyclic arrangement of water molecules, the water trimer, is not accessible with rotational spectroscopy due to the lack of a permanent dipole moment in its vibrationally averaged structure.[8,15] However, when the water trimer is bound to a solute molecule, this overall cluster is usually polar and becomes visible in pure rotational spectra. A few high-resolution molecular spectroscopy studies have explored the water trimer interacting with other molecules, illustrating that the structure of the elusive water trimer is significantly affected by the environment. Resonant ion-dip infrared spectroscopy has demonstrated that the water clusters keep a cyclic structure in the C_6H_6-$(H_2O)_{3–5}$

[*] Dr. W. Li, Dr. M. M. Quesada-Moreno, Dr. P. Pinacho, Prof. Dr. M. Schnell
Deutsches Elektronen-Synchrotron
Notkestrasse 85, 22607 Hamburg (Germany)
E-mail: melanie.schnell@desy.de
Prof. Dr. M. Schnell
Christian-Albrechts-Universität zu Kiel
Institute of Physical Chemistry
Max-Eyth-Str. 1, 24118 Kiel (Germany)
Supporting information and the ORCID identification number(s) for the author(s) of this article can be found under: https://doi.org/10.1002/anie.202013899.

clusters.[18] Rotational spectroscopy revealed that Ar-$(H_2O)_3$[21] is a prolate symmetric top with Ar located on top of the cyclic water trimer subunit. A similar arrangement was also observed for acenaphthene-$(H_2O)_3$[22] and CH_2F_2-$(H_2O)_3$.[23] Interestingly, when complexing with β-propiolactone,[24] camphor,[25] the glycoaldehyde dimer,[26] or verbenone,[27] the water trimer adopts a chain structure. In the formamide-$(H_2O)_3$ complex, all molecules, including formamide, are located almost in one plane closing a sequential cycle. It was shown that formamide can act as a substitute of two water molecules, and the formamide-$(H_2O)_3$ complex mimics the overall structure of the cyclic water pentamer.[28] The water trimer thus forms different configurations depending on the solute molecule that it interacts with, highlighting the crucial role of the interplay between the water–water and water–solute interactions. A comparison of these studies indicates that the water trimer prefers to form chains when it interacts with the solute molecule as a HB donor through a strong HB such as OH···O, otherwise it prefers the cyclic form.[18,21–28] This naturally leads to the question: Which structure will the water trimer adopt when the solute molecule offers several different docking sites simultaneously?

The synergistic interplay between different weak interactions is also a challenge for quantum-chemical calculations. Useful predictions of cluster structures require high-level calculations to provide a reliable estimation of noncovalent interactions, while, at the same time, it is important to efficiently explore the complex interaction potential energy surfaces for these clusters with many degrees of freedom. Their potential energy surface is often characterized by shallow and quasi-degenerate local minima, whose number increases with the dimensions (degrees of freedom) and the size of the molecules.[23,29–33] Therefore, experiments providing an energy ranking of different structures corresponding to local minima for a given system can also be useful for benchmarking purposes.[34,35]

Results and Discussion

Herein, we report the broadband rotational spectroscopy study of microsolvated benzophenone (Ph_2CO, $Ph = C_6H_5$) to explore the preferred binding positions of water in a stepwise procedure. Complexes with up to three water molecules were observed. In Ph_2CO, two aromatic rings are linked by a carbonyl group [Figure S1 in the Supporting Information (SI)]. The carbonyl group can interact with water via a HB, whereas any of the two π rings can act as dispersion docking sites.

To accompany the spectroscopic measurements, the initial geometries of the clusters were explored using the program CREST (conformer-rotamer ensemble sampling tool).[36] This method is efficient for searching for conformations of molecular clusters.[37] The resulting geometries were used as inputs for geometry optimizations at the B3LYP-D4/def2-TZVP level[38] of theory using the Orca program.[39] Computational details are given in the SI. In total, five isomers for Ph_2CO-H_2O, twelve isomers for Ph_2CO-$(H_2O)_2$, and 52 isomers for Ph_2CO-$(H_2O)_3$ were predicted to be real minima. We divided the Ph_2CO-$(H_2O)_3$ isomers into three types based on their binding topologies: type 1 corresponds to structures including a cyclic water trimer; type 2 structures form a cyclic tetramer via OH···O HBs between the water molecules and the oxygen atom of Ph_2CO; in the type 3 structures the water molecules form an open-looped structure (Table S14).

We employed high-resolution chirped-pulse Fourier transform microwave (CP-FTMW) spectroscopy[40,41] in the 2–8 GHz frequency region using the Hamburg COMPACT spectrometer.[42] Details on the experiment, the analysis, and the fitting procedure are given in the supporting information. A gas mixture of benzophenone and water was supersonically expanded into the vacuum chamber to produce the molecular clusters and to cool down the rotational temperature to a few Kelvin. The inherent molecular fingerprint character of rotational spectroscopy arises from the fact that even small changes in the moments of inertia significantly change the resulting molecular rotational spectrum. Thus, it is possible to differentiate between isomers, conformers, and isotopologues. Based on this advantage, molecular structures can be determined from the experimental dataset of different isotopologues without structural assumptions by solving the Kraitchman equations.[43] This method exploits the shifts in the moments of inertia upon isotopic substitution, often in natural abundance or using enriched samples, to determine the coordinates of the isotopically substituted atom in the principal axis system, allowing building up the substitution structure (r_s) atom by atom. In another approach, following a nonlinear least-squares procedure, the least-square mass-dependent geometry (r_m) can be determined by fitting partial internal coordinates based on quantum chemical structures to the observed moments of inertia.[44,45]

The rotational spectrum of the Ph_2CO monomer has been previously recorded in the 8–14 and 60–73 GHz frequency ranges.[46,47] However, no isotopically substituted data was provided, which is crucial for experimental structure determination. The strongest rotational transition of the Ph_2CO monomer in our Ph_2CO-$H_2{}^{16}O$ spectrum within 2–8 GHz had a signal-to-noise ratio (SNR) of about 3000:1 (5.6 million free induction decay (FID) acquisitions). This high SNR allowed us to assign all the ^{13}C mono-substituted isotopologues and even the ^{18}O isotopologue in natural abundances of 1.1 % and 0.2 %, respectively (Figure S1). Both r_s and $r_m^{(2)}$ structural parameters have been obtained (Table S3 and Figure S2). The torsional angle of the phenyl ring was determined to 32.3(5)° (r_s) and 31.12(9)° ($r_m^{(2)}$). No indication of internal motion was observed. This is contrary to the related diphenyl ether system,[48] pointing to a significantly higher barrier than in the diphenyl ether case.

After removing the rotational transitions belonging to the Ph_2CO monomer and its isotopologues, a significant amount of transitions still remained in the spectrum (Figure 1). A majority of these transitions could be assigned to the water complexes Ph_2CO-H_2O, Ph_2CO-$(H_2O)_2$, and Ph_2CO-$(H_2O)_3$, using the JB95 program.[49] Refined fits were obtained with the AABS suite[50] employing a standard Watson-type Hamiltonian (*S*-reduction and I^r representation[51]) as implemented in Pickett's SPFIT program.[52] Their experimental and

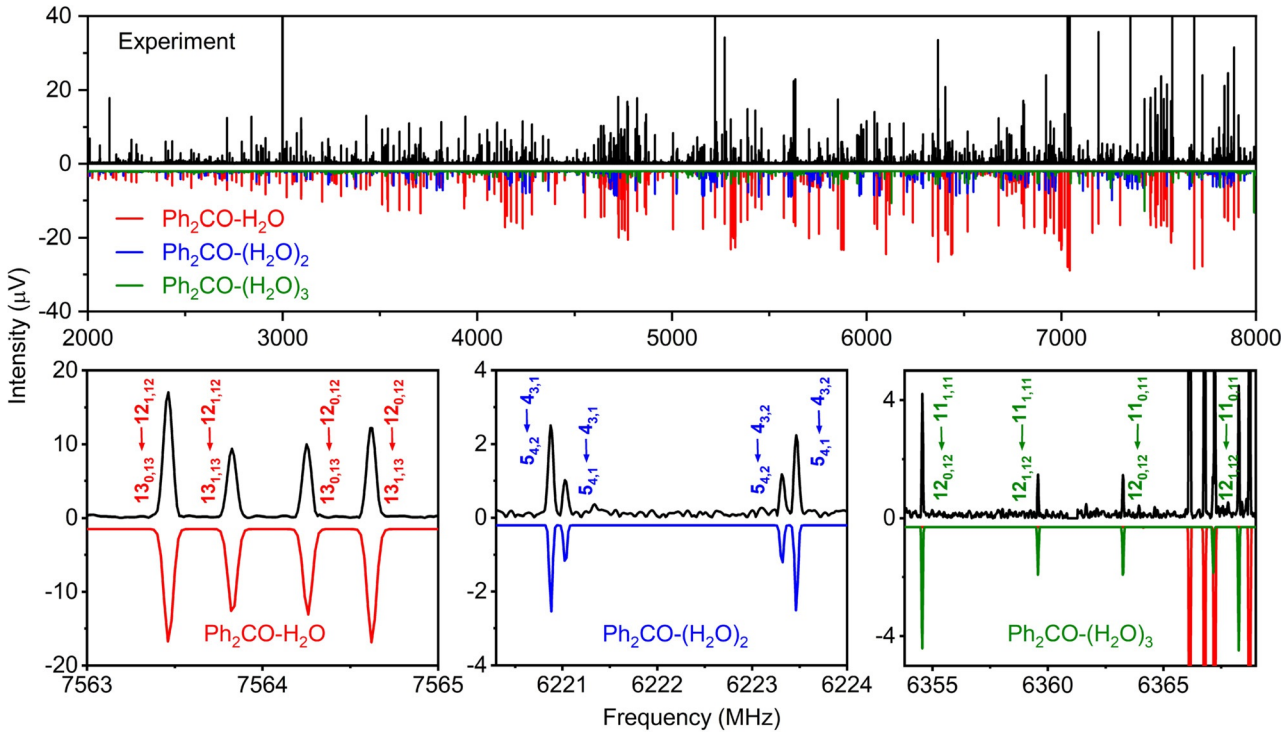

Figure 1. Broadband rotational spectrum of Ph_2CO with water. The black upper trace corresponds to the experiment (average of 5.6 million FIDs, 22 h of acquisition time). All rotational transitions arising from the Ph_2CO monomer and its isotopologues have been removed. The lower traces represent simulations produced with the experimental spectroscopic parameters, a rotational temperature of 1 K, and the theoretical dipole moment components (Table 1) for Ph_2CO-H_2O (red), Ph_2CO-$(H_2O)_2$ (blue), and Ph_2CO-$(H_2O)_3$ (green), respectively. At the bottom, parts of the spectra highlight representative transitions from each of the three complexes.

Table 1: Experimental and theoretical rotational constants of the observed Ph_2CO-$(H_2O)_{1-3}$ complexes.

	Ph_2CO-H_2O		Ph_2CO-$(H_2O)_2$		Ph_2CO-$(H_2O)_3$	
	Exp.	Theor.[a]	Exp.	Theor.	Exp.	Theor.
A [MHz]	861.76223(13)[b]	885.3(2.7%)[c]	777.88504(12)	783.9(0.8%)	649.58299(14)	667.2(2.7%)
B [MHz]	385.327992(77)	387.6(0.6%)	290.543145(51)	293.2(0.9%)	302.495306(51)	305.8(1.1%)
C [MHz]	281.465533(72)	284.8(1.2%)	226.022068(47)	225.0(0.4%)	259.646036(58)	264.4(1.8%)
D_J [kHz]	0.01048(29)		0.01117(13)		0.00806(18)	
D_{JK} [kHz]	0.05374(99)		−0.0577(10)		0.0494(15)	
D_K [kHz]	0.5056(19)		0.7326(36)		0.1443(21)	
d_1 [Hz]	−2.85(10)		−1.761(76)			
d_2 [Hz]	−1.015(35)					
$\mu_a/\mu_b/\mu_c$[d] [D]		2.7/3.1/0.5		3.7/1.9/0.9		1.1/1.4/0.1
μ_a:μ_b:μ_c[e]	1:1.3:0.1	1:1.1:0.2	1:0.4:0.3	1:0.5:0.2	1:1.4:0.0	1:1.3:0.1
σ[f] [kHz]	5.4		4.7		4.6	
N[g]	289		302		219	

[a] B3LYP-D4/def2-TZVP level of theory. [b] Standard errors within parentheses are expressed in units of the last two digits. [c] The deviation of the theoretical values from the experimental ones (in parentheses). [d] Theoretical dipole moment components. [e] The ratios of the dipole moment components. [f] Root-mean-square deviation of the fit. [g] Number of transitions in the fit.

theoretical rotational constants are collected in Table 1 and in the SI (Tables S5, S10, S15) together with all observed transitions (Tables S24–S42). No tunneling splittings arising from water motions were observed for the complexes, different to observations for other water-containing clusters.[21–23,28] In order to achieve a straightforward and unequivocal identification, we performed a second set of experiments using an isotopically enriched water sample containing about 33% $H_2{}^{18}O$ (7.3 million FID acquisitions, 28.5 hours of measurement time). All the $^{16}O/^{18}O$ water combinations were identified for Ph_2CO-H_2O and Ph_2CO-$(H_2O)_2$, providing us with the experimental structures as shown in Figure 2.

In water-containing clusters, the orientation of the OH group of the water molecule can give rise to different conformations with rather similar rotational constants, but different magnitudes of the dipole moment components. For example, the OH of the Ph_2CO-H_2O cluster can rotate out of plane and result in two minima, conformers 1 and 2

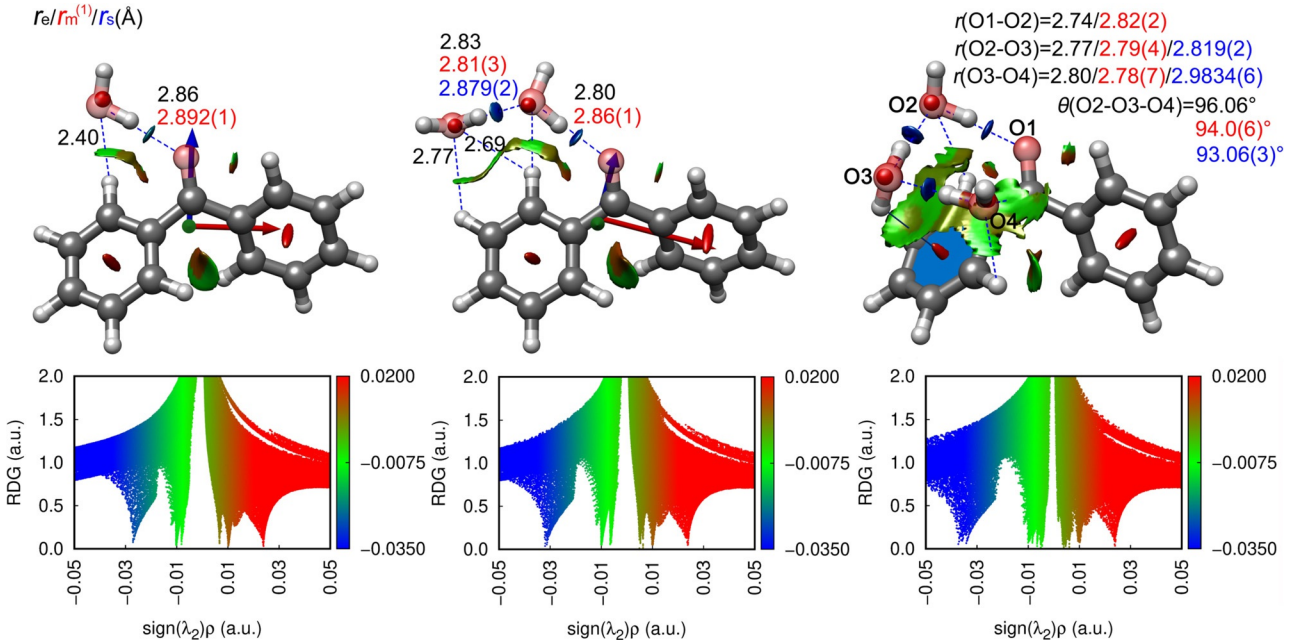

Figure 2. Structures and dominant intermolecular interactions (based on an NCI analysis, see text) of Ph_2CO-H_2O, Ph_2CO-$(H_2O)_2$, and Ph_2CO-$(H_2O)_3$. Upper panel: The experimentally determined positions of the water oxygen atoms (using the r_s method, red solid spheres) are superimposed with the calculated structures (at the B3LYP-D4/def2-TZVP level). In the NCI analysis, the gradient isosurfaces ($s = 0.5$ a.u.) are colored on a blue-green-red scale according to values of the electron density multiplied by the sign of the second Hessian eigenvalue ($\mathrm{sign}(\lambda_2)\rho$), ranging from −0.035 to 0.02 a.u. Blue indicates strong attractive interaction, green indicates weak attractive interaction, and red indicates strong repulsive interaction. The structural parameters of the hydrogen bonding network are depicted for the r_e, $r_m^{(1)}$, and r_s structures, respectively. The principal axis frames of Ph_2CO-$(H_2O)_{1-2}$ are given with relative intensities of the dipole moment components to scale ($\mu_a/\mu_b/\mu_c$ are represented as red/blue/green colors, respectively). Lower panel: Reduced density gradient (RDG) versus $\mathrm{sign}(\lambda_2)\rho$ of Ph_2CO-H_2O, Ph_2CO-$(H_2O)_2$, and Ph_2CO-$(H_2O)_3$, as obtained from the NCI analysis.

(Table S4). Interestingly, there are eight conformers for Ph_2CO-$(H_2O)_3$ with comparable rotational constants that can be interconverted by only changing the OH orientations (Table S14).

In order to identify the experimentally observed species among the isomers with similar rotational constants, we estimated the ratios of the dipole moment components by comparing the intensities of nearby rotational transitions according to the formula [Eq. (1)]:[40]

$$\mu_\alpha/\mu_\beta \approx \sqrt{I_\alpha\gamma_\beta/I_\beta\gamma_\alpha} \qquad (1)$$

Here, μ_α, μ_β represent the types of the dipole moment components (μ_a, μ_b, μ_c), I is the experimental peak intensity, and γ is the simulated intensity of the considered transitions excluding the contribution of permanent dipole moment components. We used transitions with a signal-to-noise ratio better than 5 in the 4–7 GHz frequency region. The estimated ratios μ_a:μ_b:μ_c are 1:1.3:0.1 for Ph_2CO-H_2O, 1:0.4:0.3 for Ph_2CO-$(H_2O)_2$, and 1:1.4:0.0 for Ph_2CO-$(H_2O)_3$.

Conformers 1 and 2 (Table S4) of Ph_2CO-H_2O match the experimentally identified Ph_2CO-H_2O complex both with respect to the rotational constants and the dipole moment components ratios (1:1.1:0.2 for both conformers 1 and 2). These two conformers only slightly differ in the orientations of the free OH group of the water molecule. The hydrogen atom of the free OH of conformer 1 rotates out of the *ab* plane of Ph_2CO (Figure 2), whereas that of conformer 2 is located in the *ab* plane (Table S4). Both conformers are computed to be almost isoenergetic (with and without zero-point vibrational energy (ZPVE)). The next conformer is about 4.5 kJ mol^{-1} higher in energy. To provide further information for the assignments, we calculated their planar moments of inertia P_{cc}, which indicate the mass distribution out of the *ab* inertial plane. The P_{cc} value of conformer 1 (50.11 μÅ^2) is in agreement with that of the experimentally observed Ph_2CO-H_2O complex (51.23828(56) μÅ^2), while the P_{cc} value of conformer 2 (47.68 μÅ^2) is closer to the experimental P_{cc} value of the Ph_2CO monomer (47.56578-(13) μÅ^2). Thus, we assign conformer 1 to the experimentally observed structure.

The structure of Ph_2CO-$(H_2O)_2$ can be assigned to the most stable conformer (conformer 1) by comparing the experimentally obtained rotational constants and the extracted ratios of the dipole moment components with the theoretical ones (Tables 1 and S9). The identified structures for Ph_2CO-$(H_2O)_2$ can be further confirmed with the experimental r_s and $r_m^{(1)}$ structures. We searched for the other predicted Ph_2CO-H_2O and Ph_2CO-$(H_2O)_2$ structures, but the remaining rotational transitions could not be assigned to any of the predicted Ph_2CO-H_2O and Ph_2CO-$(H_2O)_2$ isomers.

The theoretical structures (B3LYP-D4/def2-TZVP) of the Ph_2CO-$H_2O_{(1-3)}$ complexes are shown in Figure 2, with the experimentally derived atom positions superimposed. To investigate and visualize the intermolecular interactions, we

used the noncovalent interaction (NCI) approach,[53] which is based on the electron density and its derivatives. It indicates where strong HBs (blue) and weak attractive interactions (green) occur. The observed clusters consist of a network of multiple noncovalent bonds. In each case, one water moiety is anchored to the carbonyl group through an O_w–H···$O_{C=O}$ HB (in the subscript, w denotes water, C=O is the carbonyl group). For Ph_2CO-H_2O, the water molecule almost lies in the *ab* symmetry plane of the Ph_2CO monomer, as discussed, and is locked through a secondary C–H···O_w interaction, which explains the observed lack of water tunneling. For Ph_2CO-$(H_2O)_2$, the second water interacts with the first water molecule as a proton donor through an O_{w2}–H···O_{w1} HB and is reinforced by two bifurcated weak C–H···O_{w2} interactions with the two adjacent hydrogen atoms of the phenyl group, with computed distances of 2.69 Å and 2.77 Å. The distances and angles defining those intermolecular interactions have been characterized experimentally by r_s and $r_m^{(1)}$ structures. They are in good agreement with the r_e structure using the DFT-D4 method (Figures 2, S3, S6, and Tables S7, S12).

For the Ph_2CO-$(H_2O)_3$ complex, quantum-chemical calculations (B3LYP-D4/def2-TZVP level) predict eight local minima with rather similar rotational constants within a relative energy window of about 15 kJ mol^{-1} after ZPVE and basis set superposition error (BSSE) corrections (Table S14). Three of them, with corrected relative energies of 0, 4.6, and 7.3 kJ mol^{-1}, respectively, are type 3 open-looped structures. They differ from each other in the orientation of the free OH group. In the open-looped-(I) and (II) structures, an O–H···π bond between the second water and the phenyl ring is formed. In the open-looped-(III) structure, the free OH group of the second water molecule points to the opposite direction of the π ring. This last arrangement could cause a higher relative energy. The other five isomers belong to the type 1 group, in which water molecules form a cyclic trimer, with the lowest energy complex of this group being about 6.5 kJ mol^{-1} higher in energy. Their structures differ in the orientation of the hydrogen bonding network of the water trimer. Two structures adopt a clockwise (CW) and the other two a counterclockwise (CCW) orientation. For the remaining complex (15.1 kJ mol^{-1}), the two OH groups of one water molecule act as proton donors for HBs (bifurcated structure). For conciseness, only the most stable structures (open-looped-(I), (II), CW-(I), and CCW-(I)) will be discussed here (Figure 3).

Nine computational methods were employed to determine their relative energies (Figure S11). Most of them predict the open-looped-(I) structure as the global minimum, while the DLPNO-CCSD(T) method suggests the CW-(I) structure to be the most stable conformer. The B3LYP-D3(BJ)/def2-TZVP method energetically prefers the CCW-(I) structure. However, with the addition of ZPVE and BSSE corrections, all methods identify the open-looped-(I) as the global minimum (see its structure and partially structural information in Figure 2), except for the MP2/6-311++G(d,p)

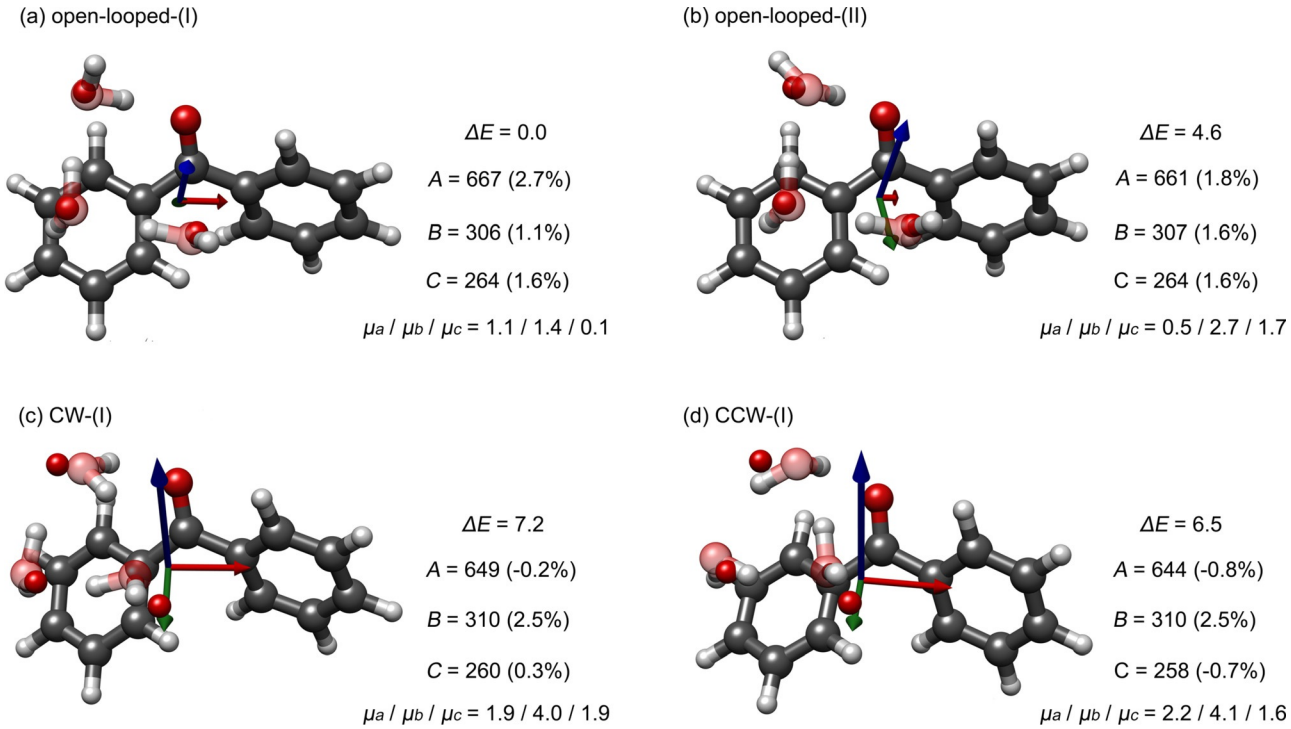

Figure 3. The most stable structures of the Ph_2CO-$(H_2O)_3$ species optimized at the B3LYP-D4/def2-TZVP level superimposed with experimentally determined r_s positions of the oxygen atoms of the water molecules (solid red spheres). The calculated rotational constants (in MHz), their deviations from the experimental values (in %, in parentheses), dipole moments (in Debye), and relative energies (in kJ mol^{-1}, with ZPVE and BSSE corrections at the B3LYP-D4/def2-TZVP level) are listed for each species. The principal axis frames are shown with relative intensities of the dipole moment components to scale (μ_a/ μ_b/ μ_c are shown as colors of red/blue/green).

method, which predicts the CCW-(I) and the open-looped-(I) structure to be quasi isoenergetic (within 0.2 kJ mol^{-1} (Tables S14 and S19).

Despite an intense search, only one Ph_2CO-$(H_2O)_3$ cluster could be identified in the spectrum. The barrier to unlock the cyclic water trimer, which means to pass from CW-(I) to open-looped-(I), is computed to be 2.1 kJ mol^{-1} (at the B3LYP-D4/def2-TZVP level, Figure S12). Most probably, this low barrier cannot prevent the cyclic water trimer from breaking its hydrogen bonding during the relaxation process upon rapid cooling in the supersonic expansion.[54] Our spectroscopic results clearly show that we observe an open-looped-(I) structure, which we thus identify as the global minimum. The following four experimental results strongly support this conclusion: Firstly, the r_s positions of the oxygen atoms agree much better with the open-looped-(I) structure than with the remaining structures (Figure 3). Secondly, both the $r_m^{(1)}$ geometry and the r_s geometry show that the two HBs in the water moiety are almost perpendicular to each other (93.98-(55)° and 93.06(3)°, respectively, Figure 2), which cannot be achieved in a cyclic arrangement (Tables S20–23). Thirdly, the measured ratios of the dipole moment components are 1:1.4:0.0 (μ_a:μ_b:μ_c), which only agree with the theoretical values (1:1.3:0.1) of the open-looped-(I). Finally, all the theoretical isomers display a strong μ_c dipole moment component except for the open-looped-(I) structure that has a μ_c value close to zero. In the experimental spectrum, no *c*-type transitions have been observed. Based on these observations, the open-looped-(I) structure can be unambiguously identified. In this structure (Figure 3(a)), the water trimer moiety has the shape of an isosceles right-angled triangle. It sits on top of one of the π-clouds and is anchored to the Ph_2CO surface via O_2–H···$O_{C=O}$, O_3–H···π, and C–H···O_4 interactions. The NCI analysis confirms the existence of these noncovalent bonds (Figure 2). Interestingly, it also indicates another interaction between O_4 and $C_{C=O}$ (Figure 2), with an O_4···$C_{C=O}$ bond length of 3.03 Å. This value is shorter than the sum of the van-der-Waals radii of the two atoms C (1.7 Å) and O (1.52 Å).[55] In order to further characterize this unexpected O···C bond, we used Bader's quantum theory of atoms in molecules (QTAIM) approach,[56] which evaluates the presence or absence of bonds stabilizing the complexes. The bond critical points (BCPs) and bond paths illustrate the interaction O_4···$C_{C=O}$ formed in the open-looped-(I) structure (Figure S14) but absent in the CCW-(I) and CW-(I) structures. This interaction, where the nucleophilic oxygen of the water molecule attacks the carbonyl carbon with a direction of about 90°, corresponds to the so-called Bürgi-Dunitz interaction.[57] This kind of interaction has received great attention, partly due to its ubiquity across chemistry and biology. For instance, it has been demonstrated to play an important role in dictating protein structures. In the investigation of the thermostability of the proline-rich protein collagen these interactions led to a robust structure despite a relatively low potential for hydrogen bonding.[57] Typically, two angles are used to characterize the trajectory of the nucleophile, the Bürgi-Dunitz (α_{BD}) and the Flippin-Lodge (α_{FL}) angle. For Ph_2CO-$(H_2O)_3$, α_{BD} and α_{FL} are experimentally determined to be around 95(1)° and 4(2)°, respectively

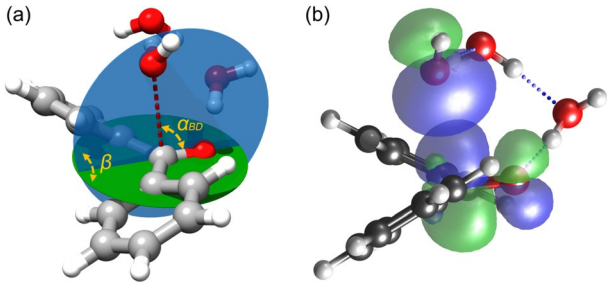

Figure 4. a) Bürgi-Dunitz trajectory and b) overlap of the n_p donor orbital of the water oxygen with the π* orbital of the carbonyl group. In panel (a), the green plane is defined by the carbonyl group and its adjacent carbon atoms, and the blue plane is defined by the oxygen atom of the third water, the carbonyl carbon atom, and the carbonyl oxygen atom. The angle between the direction of nucleophilic attack (red dashed line) and the C=O bond corresponds to α_{BD}, which is 98.5° at the B3LYP-D4/def2-TZVP level of theory, and 95(1)° in the experimental structure ($r_m^{(1)}$). The angle between the direction of nucleophilic attack and its projection on the plane perpendicular to the plane of the carbonyl group (green plane) corresponds to α_{FL}, which can be expressed with the formula $\alpha_{FL} = \text{asin}(-\sin(\alpha_{BD})\cdot\cos(\beta))$, where β is the dihedral angle defined by the blue and green planes. α_{FL} = 2.7° at the B3LYP-D4/def2-TZVP level of theory and 4(2)° in the experimental structure ($r_m^{(1)}$). The distance of nucleophilic attack is 3.08(2) Å and 3.03 Å in the experimental and theoretical structures, respectively.

(Figure 4(a)). These interactions have been discussed to result from electron donation. The Bürgi-Dunitz trajectory can maximize the overlap of the lone pair (n_p) of the nucleophile with the π* orbital of the acceptor carbonyl group. Natural bond orbital (NBO) analysis can provide insight into the n_p-π* interaction. As shown in Figure 4(b), the structure of Ph_2CO-$(H_2O)_3$ presents a large overlap between the n_p orbital of O_4 and the π* orbital of the carbonyl group with a stabilization energy of 3.6 kJ mol^{-1} (Table S17).

Conclusion

In summary, we present a rotational spectroscopy study of Ph_2CO-$(H_2O)_n$ (n = 1–3) clusters. The unambiguous identification and accurate structural parameters of these complexes are reported. When the cluster size grows from n = 1,2 to n = 3, the water bonding moiety moves from the side of the phenyl group to the top of the aromatic π cloud. For the n = 3 complex, a structure with the water trimer subunit forming an open-looped arrangement like an isosceles right-angled triangle was experimentally observed; in contrast, quantum-chemical calculations struggle to identify the global minimum among the cyclic and open-looped isomers. An additional OH···π bond and a Bürgi-Dunitz interaction stabilize the Ph_2CO-$(H_2O)_3$ complex. Our results show the importance of the synergistic effect of different kinds of noncovalent interactions in the molecular aggregation. The cooperative use of theoretical calculations and rotational spectroscopy is powerful to determine structural information of water-solute clusters and the intermolecular interactions at play. Experimental results can be used to benchmark theoretical

calculations, which in turn could facilitate the experimental analysis of new unexplored systems.

Acknowledgements

This work was financially supported by the Deutsche Forschungsgemeinschaft (SCHN1280/4-2, project number 271359857) in the context of the priority program SPP 1807 "Control of London dispersion interactions in molecular chemistry". M.M.Q.M. thanks the Fundación Alfonso Martín Escudero for a postdoctoral grant. P.P. thanks the Alexander von Humboldt Foundation for a postdoctoral fellowship. We also acknowledge the scientific exchange and support of the Center for Molecular Water Science (CMWS). Open access funding enabled and organized by Projekt DEAL.

Conflict of interest

The authors declare no conflict of interest.

Keywords: hydrogen bonding · microsolvation · rotational spectroscopy · structure elucidation · water clusters

[1] K. Müller-Dethlefs, P. Hobza, *Chem. Rev.* **2000**, *100*, 143 – 167.
[2] A. S. Mahadevi, G. N. Sastry, *Chem. Rev.* **2016**, *116*, 2775 – 2825.
[3] E. Brini, C. J. Fennell, M. Fernandez-Serra, B. Hribar-Lee, M. Lukšič, K. A. Dill, *Chem. Rev.* **2017**, *117*, 12385 – 12414.
[4] K. Morokuma, L. Pedersen, *J. Chem. Phys.* **1968**, *48*, 3275 – 3282.
[5] P. A. Kollman, L. C. Allen, *J. Chem. Phys.* **1969**, *51*, 3286 – 3293.
[6] D. Hankins, J. W. Moskowitz, F. H. Stillinger, *J. Chem. Phys.* **1970**, *53*, 4544 – 4554.
[7] T. R. Dyke, J. S. Muenter, *J. Chem. Phys.* **1974**, *60*, 2929 – 2930.
[8] N. Pugliano, R. J. Saykally, *Science* **1992**, *257*, 1937 – 1940.
[9] J. D. Cruzan, L. B. Braly, K. Liu, M. G. Brown, J. G. Loeser, R. J. Saykally, *Science* **1996**, *271*, 59 – 62.
[10] K. Liu, M. G. Brown, J. D. Cruzan, R. J. Saykally, *Science* **1996**, *271*, 62 – 64.
[11] K. Liu, J. D. Cruzan, R. J. Saykally, *Science* **1996**, *271*, 929 – 933.
[12] K. Liu, M. G. Brown, C. Carter, R. J. Saykally, J. K. Gregory, D. C. Clary, *Nature* **1996**, *381*, 501 – 503.
[13] U. Buck, I. Ettischer, M. Melzer, V. Buch, J. Sadlej, *Phys. Rev. Lett.* **1998**, *80*, 2578 – 2581.
[14] F. N. Keutsch, R. J. Saykally, *Proc. Natl. Acad. Sci. USA* **2001**, *98*, 10533 – 10540.
[15] F. N. Keutsch, J. D. Cruzan, R. J. Saykally, *Chem. Rev.* **2003**, *103*, 2533 – 2577.
[16] C. Pérez, M. T. Muckle, D. P. Zaleski, N. A. Seifert, B. Temelso, G. C. Shields, Z. Kisiel, B. H. Pate, *Science* **2012**, *336*, 897 – 901.
[17] C. Pérez, D. P. Zaleski, N. A. Seifert, B. Temelso, G. C. Shields, Z. Kisiel, B. H. Pate, *Angew. Chem. Int. Ed.* **2014**, *53*, 14368 – 14372; *Angew. Chem.* **2014**, *126*, 14596 – 14600.
[18] R. N. Pribble, T. S. Zwier, *Science* **1994**, *265*, 75 – 79.
[19] C. J. Gruenloh, J. R. Carney, C. A. Arrington, T. S. Zwier, S. Y. Fredericks, K. D. Jordan, *Science* **1997**, *276*, 1678 – 1681.
[20] W. Caminati, J.-U. Grabow, *Advancements in Microwave Spectroscopy in Frontiers and Advances in Molecular Spectroscopy* (Ed.: J. Laane), Elsevier, Amsterdam, **2018**, pp. 569 – 598.
[21] E. Arunan, T. Emilsson, H. S. Gutowsky, *J. Am. Chem. Soc.* **1994**, *116*, 8418 – 8419.
[22] A. L. Steber, C. Pérez, B. Temelso, G. C. Shields, A. M. Rijs, B. H. Pate, Z. Kisiel, M. Schnell, *J. Phys. Chem. Lett.* **2017**, *8*, 5744 – 5750.
[23] C. Calabrese, W. Li, G. Prampolini, L. Evangelisti, I. Uriarte, I. Cacelli, S. Melandri, E. J. Cocinero, *Angew. Chem. Int. Ed.* **2019**, *58*, 8437 – 8442; *Angew. Chem.* **2019**, *131*, 8525 – 8530.
[24] C. Pérez, J. L. Neill, M. T. Muckle, D. P. Zaleski, I. Peña, J. C. López, J. L. Alonso, B. H. Pate, *Angew. Chem. Int. Ed.* **2015**, *54*, 979 – 982; *Angew. Chem.* **2015**, *127*, 993 – 996.
[25] C. Pérez, A. Krin, A. L. Steber, J. C. López, Z. Kisiel, M. Schnell, *J. Phys. Chem. Lett.* **2016**, *7*, 154 – 160.
[26] C. Pérez, A. L. Steber, B. Temelso, Z. Kisiel, M. Schnell, *Angew. Chem. Int. Ed.* **2020** https://doi.org/10.1002/anie.201914888; *Angew. Chem.* **2020** https://doi.org/10.1002/ange.201914888.
[27] M. Chrayteh, A. Savoia, T. R. Huet, P. Dréan, *Phys. Chem. Chem. Phys.* **2020**, *22*, 5855 – 5864.
[28] S. Blanco, P. Pinacho, J. C. López, *J. Phys. Chem. Lett.* **2017**, *8*, 6060 – 6066.
[29] L. A. Burns, Á. Vázquez-Mayagoitia, B. G. Sumpter, C. D. Sherrill, *J. Chem. Phys.* **2011**, *134*, 084107.
[30] S. Grimme, *Wiley Interdiscip. Rev.: Comput. Mol. Sci.* **2011**, *1*, 211 – 228.
[31] W. Hujo, S. Grimme, *Phys. Chem. Chem. Phys.* **2011**, *13*, 13942 – 13950.
[32] J. Řezáč, P. Hobza, *Chem. Rev.* **2016**, *116*, 5038 – 5071.
[33] G. Prampolini, P. R. Livotto, I. Cacelli, *J. Chem. Theory Comput.* **2015**, *11*, 5182 – 5196.
[34] R. A. Mata, M. A. Suhm, *Angew. Chem. Int. Ed.* **2017**, *56*, 11011 – 11018; *Angew. Chem.* **2017**, *129*, 11155 – 11163.
[35] H. C. Gottschalk, A. Poblotzki, M. Fatima, et al., *J. Chem. Phys.* **2020**, *152*, 164303.
[36] a) S. Grimme, *J. Chem. Theory Comput.* **2019**, *15*, 2847 – 2863; b) S. Grimme, C. Bannwarth, P. Shushkov, *J. Chem. Theory Comput.* **2017**, *13*, 1989 – 2009; c) S. Grimme, C. Bannwarth, S. Dohm, A. Hansen, J. Pisarek, P. Pracht, J. Seibert, F. Neese, *Angew. Chem. Int. Ed.* **2017**, *56*, 14763 – 14769; *Angew. Chem.* **2017**, *129*, 14958 – 14964.
[37] F. Xie, N. A. Seifert, W. Jäger, Y. Xu, *Angew. Chem. Int. Ed.* **2020**, *59*, 15703 – 15710; *Angew. Chem.* **2020**, *132*, 15833 – 15840.
[38] a) E. Caldeweyher, C. Bannwarth, S. Grimme, *J. Chem. Phys.* **2017**, *147*, 034112; b) E. Caldeweyher, S. Ehlert, A. Hansen, H. Neugebauer, S. Spicher, C. Bannwarth, S. Grimme, *J. Chem. Phys.* **2019**, *150*, 154122; c) F. Weigend, R. Ahlrichs, *Phys. Chem. Chem. Phys.* **2005**, *7*, 3297 – 3305.
[39] Orca Version 4.0.1, F. Neese, *Wiley Interdiscip. Rev.: Comput. Mol. Sci.* **2012**, *2*, 1, 73 – 78.
[40] G. G. Brown, B. C. Dian, K. O. Douglass, S. M. Geyer, S. T. Shipman, B. H. Pate, *Rev. Sci. Instrum.* **2008**, *79*, 053103.
[41] G. B. Park, R. W. Field, *J. Chem. Phys.* **2016**, *144*, 200901.
[42] D. Schmitz, V. Alvin Shubert, T. Betz, M. Schnell, *J. Mol. Spectrosc.* **2012**, *280*, 77 – 84.
[43] J. Kraitchman, *Am. J. Phys.* **1953**, *21*, 17 – 24.
[44] J. K. G. Watson, A. Roytburg, W. Ulrich, *J. Mol. Spectrosc.* **1999**, *196*, 102 – 119.
[45] Z. Kisiel, *J. Mol. Spectrosc.* **2003**, *218*, 58 – 67.
[46] A. Maris, S. Melandri, W. Caminati, P. G. Favero, *Chem. Phys. Lett.* **1996**, *256*, 509 – 512.
[47] C. West, G. Sedo, J. Wijngaarden, *J. Mol. Spectrosc.* **2017**, *335*, 43 – 48.
[48] M. Fatima, A. L. Steber, A. Poblotzki, C. Pérez, S. Zinn, M. Schnell, *Angew. Chem. Int. Ed.* **2019**, *58*, 3108 – 3113; *Angew. Chem.* **2019**, *131*, 3140 – 3145.
[49] D. F. Plusquellic, JB95, Spectral Fitting Program, **2001**.
[50] Z. Kisiel, L. Pszczolkowski, I. R. Medvedev, M. Winnewisser, F. C. De Lucia, E. Herbst, *J. Mol. Spectrosc.* **2005**, *233*, 231 – 243.
[51] J. K. G. Watson, in *Vibrational Spectra and Structure*, *Vol. 6* (Ed.: J. R. Durig), Elsevier, New York, Amsterdam, **1977**, pp. 1 – 89.

[52] H. M. Pickett, *J. Mol. Spectrosc.* **1991**, *148*, 371 – 377.
[53] E. R. Johnson, S. Keinan, P. Mori-Sánchez, J. Contreras-García, A. J. Cohen, W. Yang, *J. Am. Chem. Soc.* **2010**, *132*, 6498 – 6506.
[54] R. S. Ruoff, T. D. Klots, T. Emilson, H. S. Gutowski, *J. Chem. Phys.* **1990**, *93*, 3142 – 3150.
[55] A. Bondi, *J. Phys. Chem.* **1964**, *68*, 441 – 451.
[56] R. F. W. Bader, *Atoms in Molecules: A Quantum Theory*, Oxford University Press, Oxford, **1994**.
[57] a) H. B. Bürgi, J. D. Dunitz, E. Shefter, *J. Am. Chem. Soc.* **1973**, *95*, 5065 – 5067; b) R. W. Newberry, R. T. Raines, *Acc. Chem. Res.* **2017**, *50*, 1838 – 1846.

Manuscript received: October 15, 2020
Version of record online: January 25, 2021

